

# “Finding” a Pulse Shape

Jason M. Taylor

May 16, 2005

## Introduction

“The laser cavity finds the pulse that minimizes loss—it’s like magic.” The dynamics of pulses in a Kerr Lens Mode-Locked laser converge to a steady stream of ultrafast pulses. Here we attempt to discover the function that the laser cavity minimizes.

This paper is organized into three parts. First we introduce KLM lasers and review the physics of the KLM cavity, then we examine the dynamics of laser using numerical simulation, and finally we use an analytic approach to discover the function that the pulse is minimizing.

## 1 Kerr Lens Mode-Locked Lasers

Kerr lens mode-locked (KLM) lasers were first realized in 1991 [14]. This laser had pulse width of 60 femtoseconds. Lasers producing pulses this short are known as ultrafast lasers. At this time scale, most molecular dynamics are frozen. Molecules do not spin, vibrate, or even emit light at a rate faster than these laser pulses. This makes ultrafast lasers a invaluable tool for studying molecular dynamics [16].

KLM lasers mode-lock when self-focusing in the Kerr medium causes the loss in a cavity to decrease with increasing pulse power. Shorter pulses experience less loss and therefore more net gain. This feedback causes mode-locking of many frequencies in phase with each other resulting in an ultrashort pulse. Using a Ti:Sapphire ( $\text{Ti:Al}_2\text{O}_3$ ) crystal as both the gain medium and the Kerr medium as been successful and popular. The pulse reaches a steady state solution when the

pulse shortening effect of the fast saturable absorber is balanced by pulse lengthening effects such as dispersion or bandwidth filtering. The soliton-like pulse that is formed is a result of a balance between GVD, SPM. Gain saturation, bandwidth filtering, and the pulse shortening effect of the Kerr media stabilize the pulse.

## 1.1 Mode-locking

The term ‘Mode-locking’ refers to the frequency modes in a laser cavity. Typically we think of a short laser pulse in the time domain. A Gaussian laser pulse in the time domain is a Gaussian shape in the frequency domain. Constructing a laser cavity to excite nearby cavity modes in phase with each other is the art of mode-locking.

Kerr Lens Mode-Locked lasers operate by passive mode-locking with a fast saturable absorber. The theoretical foundation of these lasers was first developed by Herman Haus in 1975 [4]. The science of short laser pulses lasers has progressed steadily over the last 30 years. Figure 1 shows progress by pulse width, year, and material. This paper focuses on the most popular development of the last ten years of mode-locking, Kerr-Lens Mode-locking using Ti:Sapphire.

## 1.2 Fast Saturable Absorber Mode-locking

A fast saturable absorber has an absorption recovery time that is fast compared to the width of the pulse. Figure 2 shows the recovery of the absorption. Unlike a slow saturable absorber [5] we assume that the gain is constant over the duration of the pulse. The fast recovery of the absorption shortens the trailing edge of the pulse.

The fast saturable absorber loss is modeled by

$$s(t) = \frac{s_0}{1 + I(t)/I_{\text{sat}}}$$

where  $s_0$  is the unsaturated loss,  $I(t)$  is the intensity of the pulse, and  $I_{\text{sat}}$  is the saturation intensity of the absorber.

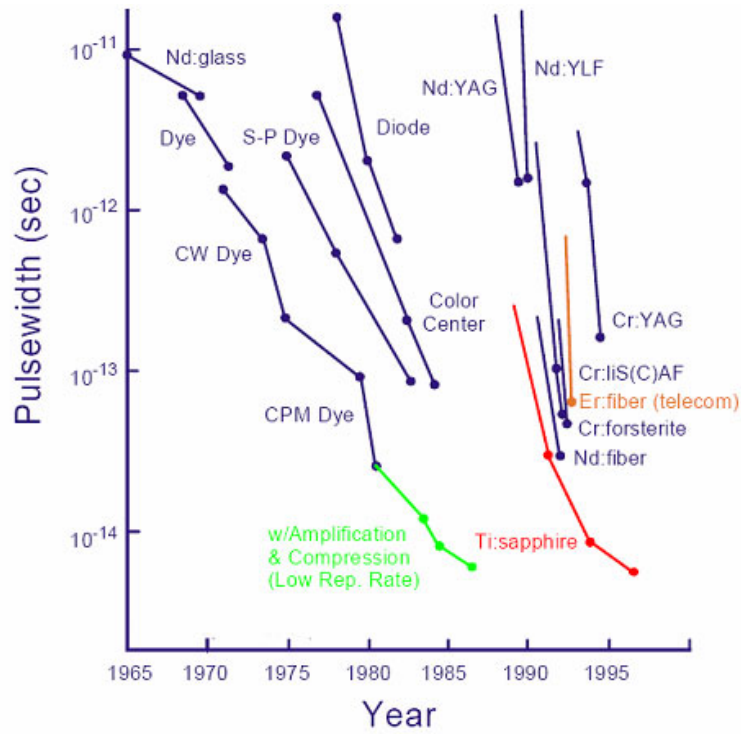


Figure 1: Pulsewidths by year and material [5].

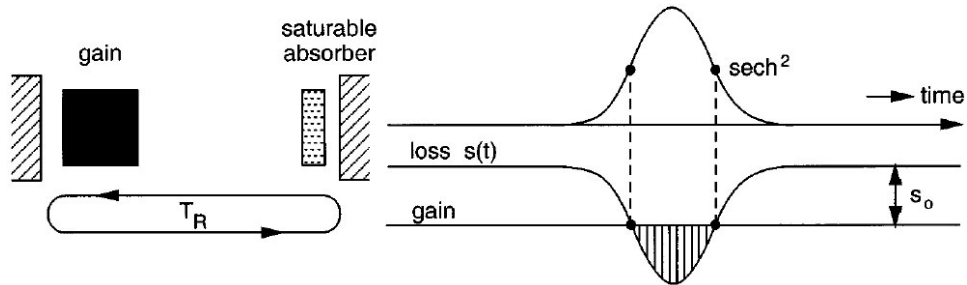


Figure 2: Fast Saturable Absorber [5]

Following Haus [5], if the saturation is weak we can expand this to

$$s(t) = s_0 - s_0 \frac{I(t)}{I_{\text{sat}}}.$$

If we normalize  $|a(t)|^2$  to be power then we can write

$$s(t) = s_0 - \frac{s_0 |a(t)|^2}{I_{\text{sat}} A_{\text{eff}}} \equiv s_0 - \gamma |a(t)|^2$$

where  $\gamma$  is called the self amplitude modulation (SAM) coefficient.

Haus' master equation balances gain, loss, gain bandwidth filtering, and the saturable absorber.

$$\frac{1}{T_R} \frac{\partial}{\partial T} a = (g - l)a + \frac{g}{\Omega_g^2} \frac{\partial^2}{\partial t^2} a - (s_0 - \gamma|a|^2)a \quad (1)$$

We can combine  $s_0$  into  $l$

$$\frac{1}{T_R} \frac{\partial}{\partial T} a = (g - l)a + \frac{g}{\Omega_g^2} \frac{\partial^2}{\partial t^2} a + \gamma|a|^2 a. \quad (2)$$

Later we will expand gain bandwidth broadening term,  $g/\Omega_g^2$ , to include cavity bandwidth filtering and call these dispersive effects  $D_{gf}$  where  $D_{gf} = g/\Omega_g^2 + 1/\Omega_f$ .

The solution to this master equation (2) is

$$a_0(t) = A_0 \operatorname{sech}(t/\tau), \quad (3)$$

where

$$\frac{1}{\tau^2} = \frac{\gamma A_0^2 \Omega_g^2 a}{2g}$$

and

$$l - g = \frac{g}{\Omega_g^2 \tau^2} \quad (4)$$

By inspection of (2) and (3) we can see that this analytical solution is unbounded. Gain saturation must be introduced into the model to arrive at a stable pulse. Equation 4 is also a bit confusing at first glance. Typically for laser operation we would assume that gain  $g$  would be larger than loss  $l$  making Equation 4 false. This equation applies for noise in the cavity during pulsed operation. We have negative net gain for noise. A short pulse by way of Self Amplitude Modulation sees less loss through the saturable absorber and therefore positive net gain.

The pulse shortening per pass is given by [7]:

$$\frac{\Delta\tau}{\tau} = \frac{\gamma W}{2\tau} \quad (5)$$

The PSR given in (5) shows an increase in pulse shortening with shorter pulses. For a fast saturable absorber the pulse shortening rate increases as  $\tau$  gets smaller ( $1/\tau$ ). We will find that for a fast saturable absorber the final evolution of our ultrashort pulses will be dominated by soliton effects.

This inverse- $\tau$  relationship has one drawback. For long pulses the pulse shortening rate is small. This is the primary reason most fast saturable mode-locked lasers are not self-starting and need to be started by perturbing the cavity in some way. A short pulse is necessary to get the pulse shortening started.

### 1.2.1 Kerr Lens Mode-locking

Kerr lens mode-locked lasers operate by an artificial fast saturable absorber caused by the combination of Kerr lensing and an aperture to give a near instantaneous response time much faster than pulse widths.

The Kerr effect causes the refractive index of a medium to increase with intensity:

$$n(I) = n_0 + n_2 I$$

where

$$n_0 = 1.76, n_2 = 3 \times 10^{-20} \text{ m}^2\text{W}^{-1}$$

for Ti:Sapphire.

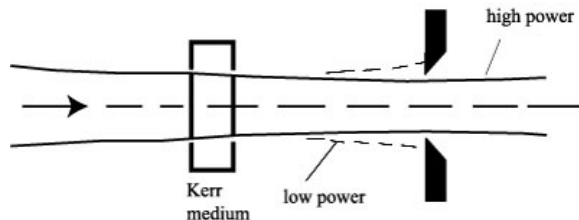


Figure 3: Kerr medium and aperture.

We assume the spatial mode of the pulse is Gaussian. The center of the pulse has a higher intensity than the outer part. When the pulse goes through the Kerr medium in the cavity, the

center sees a greater index of refraction than the outer part. This causes a focusing that is dependent on total pulse intensity. By putting an aperture in the cavity that is smaller than the CW pulse width we can encourage shorter more intense pulses (Fig. 3). The net effect of the Kerr media and the aperture creates a fast saturable absorber. ABCD-matrix beam propagation can be used to describe this self-focusing [6].

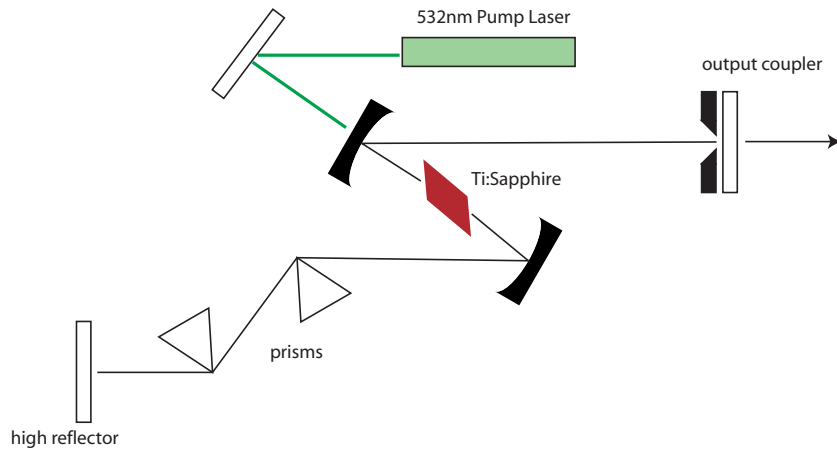


Figure 4: KLM Cavity

The Ti:Sapphire KLM oscillator design from 1991 has remained largely unchanged. Figure 4 shows the Ti:Sapphire crystal pumped at 532nm. The Titanium doped Sapphire crystal acts as both the gain medium and the Kerr medium. The Kerr focusing in combination with either a real aperture, cavity misalignment, or pump/cavity beam overlap forms the artificial fast saturable absorber. The two prisms are included to compensate for the positive group velocity dispersion (GVD) caused during propagation through the Ti:Sapphire crystal. More recent cavity designs use chirped mirrors to compensate for Third Order Dispersion (TOD) and GVD rather than prisms. An acusto-optic modulator is sometimes added in the cavity to initiate mode-locking.

### 1.3 Soliton Effects

Ultrashort pulses propagating in a medium typically experience Group Velocity Dispersion. The broad bandwidth frequency components of a transform limited pulse experience an index of refraction based on their frequency  $n(\omega)$ . This causes the red side of the pulse to get ahead of the blue side of the pulse in the case of normal dispersion. This is called a positive chirp. In the case of anomalous dispersion the blue side of the pulse propagates faster than the red resulting in a negatively chirped pulse. This chirping causes the pulse to become broader in time but the frequency spectrum remains unchanged.

If we can apply group velocity dispersion (GVD) to our pulse

$$\Delta a = jD \frac{d^2}{dt^2} a.$$

Most materials have normal dispersion which induce a positive chirp. In a KLM cavity it is essential to compensate for this positive chirp with negative dispersion. Negative group velocity dispersion can be made using a pair of prisms [3] or diffraction gratings [15]. This balance between the positive dispersion of the cavity elements and the negative dispersion of the prism configuration allows for near zero net dispersion.

Self-Phase Modulation (SPM) changes the phase of a pulse according to the instantaneous pulse intensity. In a Kerr medium the phase will be delayed more for higher intensity.

$$\Delta a = -j\delta|a|^2 a$$

$$n(I) = n_0 + n_2 I$$

where  $n_0 = 1.76$  and  $n_2 = 3 \times 10^{-20} \text{ m}^2 \text{W}^{-1}$  for Ti:Sapphire.

Our full master equation is

$$\frac{1}{T_R} \frac{\partial}{\partial T} a = (g - l)a + \left( \frac{g}{\Omega_g^2} + \frac{1}{\Omega_f^2} + jD \right) \frac{\partial^2}{\partial t^2} a + (\gamma - j\delta)|a|^2 a \quad (6)$$

where  $g$  is gain,  $l$  is loss,  $\Omega_g$  is gain filtering,  $\Omega_f$  is cavity filtering,  $D$  is the GVD parameter,  $\gamma$  is the SAM coefficient,  $\delta$  is the SPM coefficient.

## 2 Numerical Simulation

We use the master equation approach [4, 5, 9, 8] to simulate the dynamics of a KLM oscillator. The master equation describes passive mode-locking using fast saturable absorbers and includes Group Velocity Dispersion (GVD), Self-Amplitude Modulation (SAM), Self-Phase Modulation (SPM), and bandwidth filtering. Most oscillator dynamics that are not explicitly dependent on spatial modes can be included in this model.

Our simulations are seeded with a Gaussian pulse in the picosecond to 100 femtosecond range. The master equation governs the pulse evolution simulating one cavity round-trip of the pulse for each time step. Typical simulations converge on a steady state solution within 2,000 to 8,000 round trips. The non-linear and dispersive effects were applied to the pulse using the Split-Step Fourier Transform method [1]. This numerical method is commonly used to simulate intense pulses propagating in optical fiber.

### 2.1 Simulation Procedure

The simulator is a relatively simple implementation of the pulse evolution described in Haus' master equation (7). The split-step Fourier transform method was used to evolve a pulse through one round trip of cavity. We apply the linear cavity effects in the frequency domain and we apply the non-linear saturation and phase modulation effects in the time domain.

$$\frac{1}{T_R} \frac{\partial}{\partial T} A(T, t) = (g - l)A(T, t) + \left( D_{gf} + jD \right) \frac{\partial^2}{\partial t^2} A(T, t) + (\gamma - j\delta) |A(T, t)|^2 A(T, t) \quad (7)$$

Haus' Master Equation (7) from left to right has a net gain term  $(g-l)$ , dispersion  $D$ , bandwidth filtering  $D_{gf}$  where  $D_{gf} = g/\Omega_g^2 + 1/\Omega_f^2$ , the SAM coefficient  $\gamma$ , and  $\delta$  the Self Phase Modulation (SPM) coefficient.



Generally the combination of gain and SAM produce the ultrashort pulse and keep it stable while GVD and SPM shorten it further.

At the core of this simulation is the split-step Fourier method.

We've adapted Agrawal's [1] use of the SSFM in pulse propagation in optical fiber to our master equation describing a KLM cavity. In the fiber derivation, the length of the fiber is broken down into a large number of segments and then the dispersive terms and nonlinear terms are applied separately to each segment. If we view our master equation in the form,

$$\frac{\partial A}{\partial T} = (\hat{D} + \hat{N})A, \quad (8)$$

we have linear terms,

$$\hat{D} = g - l + (D_{gf} + jD) \frac{\partial^2}{\partial t^2}, \quad (9)$$

and the nonlinear terms,

$$\hat{N} = (\gamma - j\delta)|A|^2. \quad (10)$$

We assume that the dispersive terms and non-linear terms can be applied to the pulse separately. We also assume that effects of one round trip on a pulse are small so we can apply the operators in one step rather than breaking up the cavity into several segments.

We seed our simulations with a relatively broad bandwidth low intensity pulse. In physical KLM oscillators it is usually necessary to perturb the cavity by moving one of the dispersion compensating prisms in order to seed the cavity with something pulse-like to feedback on. Fast saturable absorber oscillators are typically not self starting since the pulse shortening rate is weak for long pulses and successively stronger for short pulses.

We assume that that the population lifetime of our gain medium is long compared to the repetition rate of the cavity. This means that the gain will saturate according to the average power over many pulses rather than over a single pulse width. To accommodate this assumption we calculate the effective gain between cavity round trips. In each of the cavity round trip iterations

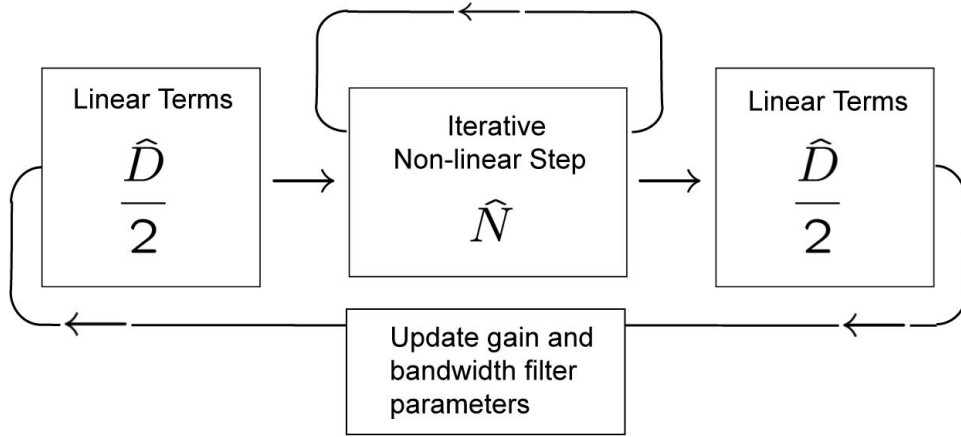


Figure 5: Simulator Block Diagram

we calculate a new gain  $g$  according to:

$$g(T) = \frac{g_0}{1 + \frac{E_P(T)}{E_{sat}}}$$

where

$$E_P(T) = \int_{-\infty}^{+\infty} |A(T, t)|^2 dt$$

$$E_P(T) = \Delta t \sum_{n=0}^N |A(T, n)|^2$$

Dispersion due to gain bandwidth and cavity bandwidth is also updated

$$D_{gf} = g/\Omega_g^2 + 1/\Omega_f^2$$

The block diagram in Figure 5 shows the operation of the simulator. For each cavity round-trip we apply linear terms to the pulse envelope in the frequency domain. Then apply the non-linear operations in the time domain and iterate until we arrive at a self-similar pulse envelope. During the outer portion of the loop the gain is adjusted to account for gain depletion.

Parameter	Value	Description
$l$	0.025	loss
$g_0$	0.0 - 0.10	unsaturated gain (0.07 typical)
$\Omega_g$	$2\pi \cdot 43$ THz	gain bandwidth
$q_0$	0.01	$s_0$ unsaturated absorber loss

Table 1: Table of simulator parameters for Ti:Sapphire [9].

## 2.2 Ti:Sapphire

We calculated our Ti:Sapphire model parameters assuming a 50fs pulse, 400mW ML output power, 90MHz repetition rate, and a 3% output coupler. We used a 14W intra-cavity power or  $1.55 \times 10^{-7}$  J/pulse corresponding to a pulse amplitude of  $A_0 = 1250$  assuming a sech pulse.

$$a_0(t) = A_0 \operatorname{sech}(t/\tau),$$

Our simulation should be sensitive to our initial gain parameter  $g_0$ . Below some threshold our net gain should be negative and above some turn-on threshold we should see a net gain. Figure 6 shows the final pulse from 20 simulations at gain values from  $g_0 = 0$  to  $g_0 = 0.2$ .

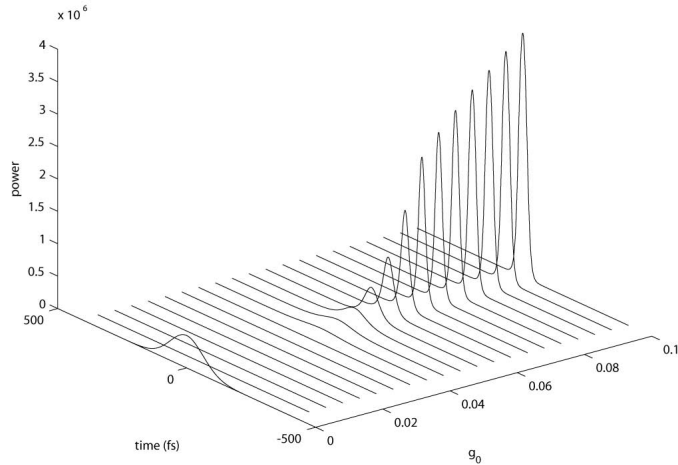


Figure 6: job24: Ti:Sapphire, Converged pulse after 8000 iterations for unsaturated gain values from 0 to 0.10, no SPM, no GVD

We can see the net gain turning positive at around  $g_0 = 0.05$ . This threshold is consistent with Figure 3 in Kaertner [8]. Each trace represents 8,000 iterations of the master equation. All pulses converged to a steady state value within this time. Last year's Matlab computer took about 5 minutes to run each simulation for a given  $g_0$ .

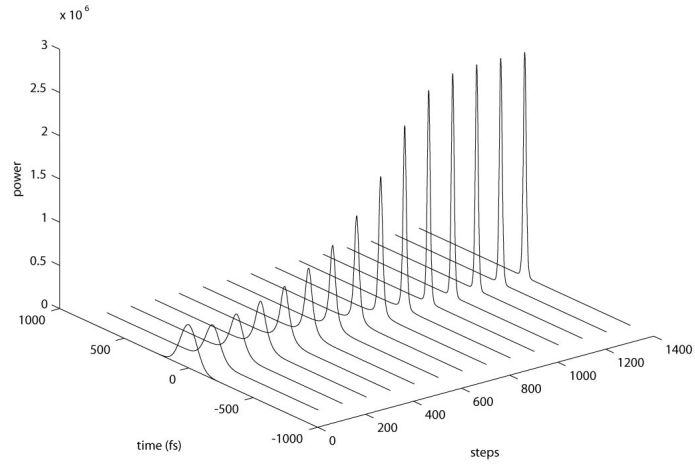


Figure 7: job40: Ti:Sapphire, Pulse evolution of an ultrashort pulse.

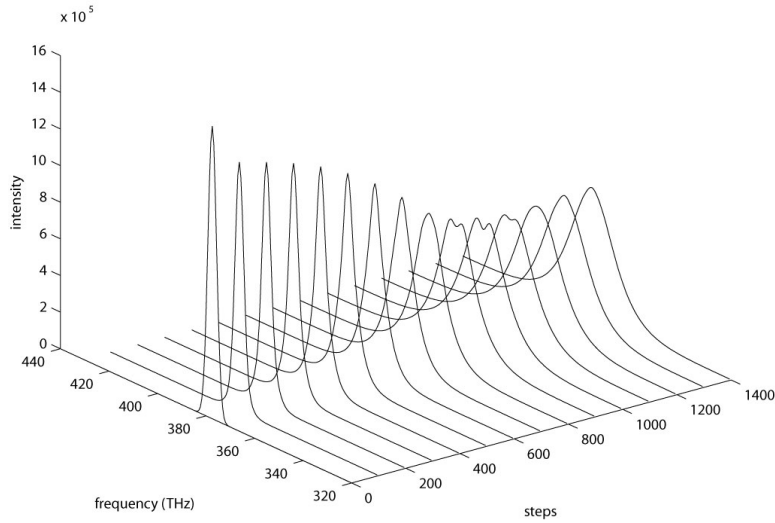


Figure 8: job40: Ti:Sapphire, Bandwidth evolution of an ultrashort pulse.

Group velocity dispersion and self phase modulation were added to the simulation. To view the

pulse evolution we saved traces every 100 simulation steps. The evolution of an ultrafast pulse is shown in Figure 7. Our initial pulse seed pulse is shown at step 0. For this simulation we seeded the simulation with a relatively short 200fs pulse. The simulations converged to their steady state pulse regardless of initial pulse width or intensity. The final pulse had a width of 38fs. This simulation converged to a steady state solution after only 1500 cavity round trips. We ran the simulation for a few thousand iterations beyond this point to confirm convergence.

The evolution of the frequency components of these pulses is shown in Figure 8. Again, the initial pulse is at step 0. The pulse evolution is easily divided up into three stages. Initially, for the first 300 steps, unsaturated gain is the dominant effect. The net gain anything other than an intense pulse is negative. Gain is followed up by self amplitude modulation shortening the pulse. The gain is eventually saturated and the self amplitude modulation effect reaches its minimum saturable loss. At around step 800 soliton effects further shorten the pulse. The dip in the middle of the pulse at step 1000 is due to self phase modulation that is eventually removed by group velocity dispersion.

### 3 Analytic Examination

Here we will attempt to find the function that the laser minimizes while ringing-up. Ideally we would like to discover a Lyapunov-like function—a monotonically decreasing, positive definite function.

#### 3.1 Complex Ginzburg-Landau Equation

The Haus master equation (6) describing the full KLM dynamics including soliton effects is a complex Ginzburg-Landau equation (CGLE). For each cavity round-trip the gain parameter  $g$  is fixed. Gain depletion attenuates the gain parameter as the total energy in the pulse approaches the limit of the gain media  $E_{sat}$ .

$$g(T) = \frac{g_0}{1 + \frac{E_P(T)}{E_{sat}}}$$

where

$$E_P(T) = \int_{-\infty}^{+\infty} |A(T, t)|^2 dt$$

This changing parameter of our non-linear partial differential equation makes solving the full ring-up dynamics difficult. It is usually difficult to find an analytic solution to the CGLE for any particular set of parameters. To simplify this analysis we will consider only the dynamics of the laser near full pulse energy  $\delta g \rightarrow 0$ .

Our complex Ginzburg-Landau equation describing the laser dynamics around the stationary solution is:

$$\frac{\partial}{\partial T} A(T, t) = (g - l)A + \left( D_{gf} + jD \right) \frac{\partial^2}{\partial t^2} A + (\gamma - j\delta)|A|^2 A \quad (11)$$

This equation has a soliton-like solution [10]

$$a(t) = A_0 \operatorname{sech}^{(1+j\beta)} \left( \frac{t}{\tau} \right),$$

and a continuous wave solution

$$a(t) = A_0 \exp(-j\omega t).$$

The CGLE:

$$\frac{\partial}{\partial T} A = A + (1 + jc_1) \frac{\partial^2}{\partial t^2} A - (1 + jc_2)|A|^2 A \quad (12)$$

The competition between these two lasing modes and relative stability of each determines whether the laser is self-starting or not. Where self-starting implies an immediate ring-up to the soliton-like solution. Soto-Crespo et. al. have extensively studied the CGLE approximated around the soliton and the CW solutions [13, 12]. Their analysis used a numerical simulation similar to the one presented earlier. They found regions of the CGLE parameter space where the CW lasing mode was unstable and the soliton lasing mode was stable which suggests that the laser should be “self-starting” in that region.

An analytic Lyapunov functional for the CW lasing mode has been reviewed and confirmed numerically [11]. Unfortunately this treatment of the CGLE did not consider soliton solutions. In the full parameter space the solitons are usually unstable and much of the space is chaotic. Rederiving the work in that paper to approximate soliton solutions is presently beyond the scope

of this author.

We will attempt to further simplify the master equation.

### 3.2 Non-linear Schrodinger Equation

As we saw in the numerical section of this paper as the pulses get shorter the soliton effects begin to dominate. For ultrashort pulses we could consider the soliton effects as the primary dynamics and assume that gain, SAM, and filtering can be considered small perturbations.

$$\frac{\partial}{\partial T}A(T, t) = jD\frac{\partial^2}{\partial t^2}A - j\delta|A|^2A \quad (13)$$

Terms this equation is identical to solitons propagating down a fiber. It has no dissipative terms so the total energy in the pulse will remain constant. This equation is known as the Non-Linear Schrodinger Equation (NLSE).

We have now restricted ourselves to an area very near the stationary solution to the Haus master equation. The Lyapunov function for this equation is well known [2]. Adapted for our NLSE parameters we a Lyapunov function.

$$V = \int_{-\infty}^{+\infty} dt \left[ -D|A|^2 + \frac{1}{2} \frac{\delta}{2} |A|^4 + \left| \frac{\partial}{\partial t} A \right|^2 \right]$$

### 3.3 Numerical Confirmation

This Lyapunov function is nothing great. We found a fractal.

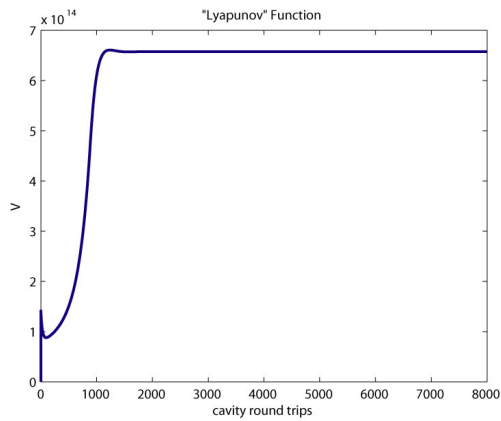


Figure 9: job89b\_1: The Lyapunov function derived from the NLSE for the CGLE.

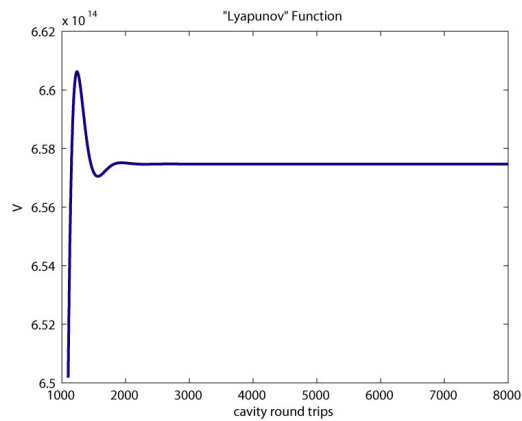


Figure 10: job89b\_2: The Lyapunov function derived from the NLSE for the CGLE.

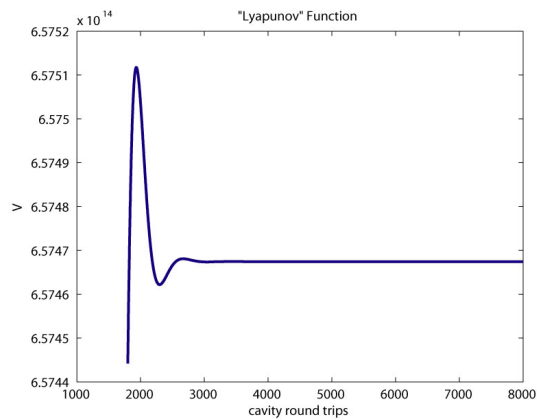


Figure 11: job89b\_3: The Lyapunov function derived from the NLSE for the CGLE.



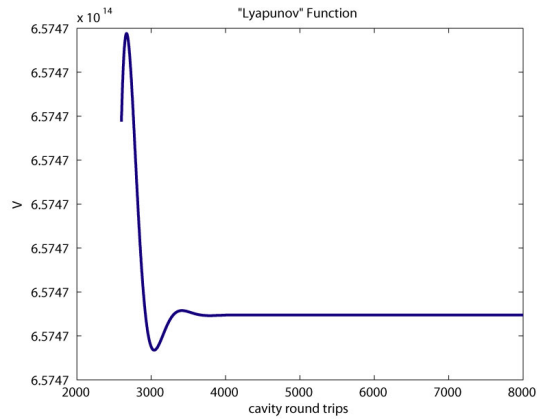


Figure 12: job89b\_4: The Lyapunov function derived from the NLSE for the CGLE.

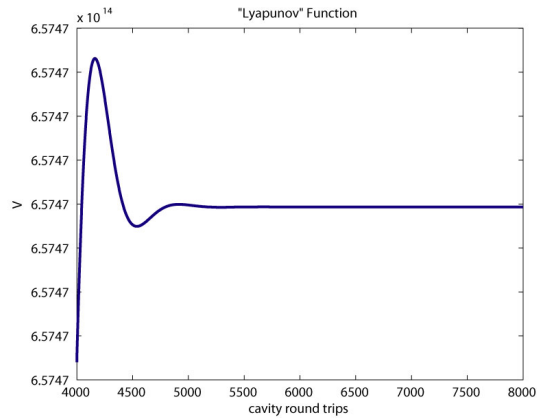


Figure 13: job89b\_2: The Lyapunov function derived from the NLSE for the CGLE.

## References

- [1] Govind P. Agrawal. *Nonlinear Fiber Optics*. Academic Press, third edition, 2001. ISBN 0120451433.
- [2] Igor S. Aranson and Lorenz Kramer. The world of the complex Ginzburg-Landau equation. *Reviews of Modern Physics*, 74:99–143, 2002.
- [3] R.L. Fork, O. E. Martinez, and J. P. Gordon. Negative dispersion using pairs of prisms. *Opt. Lett.*, 9:150, 1984.  
URL [http://jafar.media.mit.edu/library/lasers/misc/linear\\_pulse/84.05.fork.pdf](http://jafar.media.mit.edu/library/lasers/misc/linear_pulse/84.05.fork.pdf)
- [4] Herman A. Haus. Theory of mode locking with a fast saturable absorber. *J. Appl. Phys.*, 46:3049–3058, 1975.  
URL <http://jafar.media.mit.edu/library/lasers/misc/haus/75.02.haus.pdf>

- [5] Herman A. Haus. Mode-Locking of Lasers. *IEEE Journal on Selected Topics in Quantum Electronics*, 6(6):1173, 2000.  
URL <http://jafar.media.mit.edu/library/lasers/klm/00.12.haus.pdf>
- [6] Joachim Herrmann. Theory of Kerr-lens mode locking: role of self-focusing and radically varying gain. *J. Opt. Soc. Am. B*, 11(3):498, 1994.  
URL <http://jafar.media.mit.edu/library/lasers/modeling/94.03.herrmann.pdf>
- [7] E. P. Ippen. Principles of Passive Mode Locking. *Appl. Phys. B*, 58:159–170, 1994.  
URL <http://jafar.media.mit.edu/library/lasers/ultrafast/94.00.ippen.pdf>
- [8] F.X. Kartner, Juerg Aus der Au, and U. Keller. Mode-Locking with Slow and Fast Saturable Absorbers—What’s the Difference? *IEEE Journal on Selected Topics in Quantum Electronics*, 4(2):159–168, March 1998.  
URL <http://jafar.media.mit.edu/library/lasers/modeling/98.03.kartner.derAu.Keller.pdf>
- [9] F.X. Kartner, I.D. Jung, and U. Keller. Soliton Mode-Locking with Saturable Absorbers. *IEEE Journal on Selected Topics in Quantum Electronics*, 2(3):540–556, September 1996.  
URL <http://jafar.media.mit.edu/library/lasers/modeling/96.09.kartner.jung.keller.pdf>
- [10] O. E. Martinez, R.L. Fork, and J. P. Gordon. Theory of passively mode-locked lasers including self-phase modulation and group-velocity dispersion. *Opt. Lett.*, 9:156–158, 1984.  
URL [http://jafar.media.mit.edu/library/lasers/mode\\_locking/84.05.martinez.fork.gordon.pdf](http://jafar.media.mit.edu/library/lasers/mode_locking/84.05.martinez.fork.gordon.pdf)
- [11] R. Montagne, E. Hernandez-Garcia, and M. San Miguel. Numerical Study of a Lyapunov functional for the Complex Ginzburg-Landau Equation. <http://xxx.lanl.gov/abs/cond-mat/9508115>, 1995.  
URL <http://jafar.media.mit.edu/library/lasers/stability/95.08.montagne.hernandez-garcia.miguel.pdf>
- [12] J.M. Soto-Crespo, N. Akhmediev, and V. Afanasjev. Stability of the pulselike solutions of the quintic complex Ginzburg-Landau equation. *J. Opt. Soc. Am. B*, 13(7):1439–1449, 1996.  
URL <http://jafar.media.mit.edu/library/lasers/cgle/96.07.soto-crespo.akhmediev.afanasjev.pdf>
- [13] J.M. Soto-Crespo, N. Akhmediev, and G. Town. Continuous-wave versus pulse regime in a passively mode-locked laser with a fast saturable absorber. *J. Opt. Soc. Am. B*, 19(2):234–242, 2002.  
URL <http://jafar.media.mit.edu/library/lasers/modeling/02.02.soto-crespo.akhmediev.town.pdf>
- [14] D.E. Spence, P.N. Kean, and W. Sibbett. 60-fsec pulse generation from a self-mode-locked Ti:sapphire laser. *Optics Letters*, 16:42–44, 1991.  
URL <http://jafar.media.mit.edu/library/lasers/klm/91.01.spence.pdf>

- [15] Edmond B. Treacy. Optical Pulse Compression With Diffraction Gratings. *IEEE Journal of Quantum Electronics*, 5(9):454, 1969.  
URL <http://jafar.media.mit.edu/library/lasers/misc/69.09.treacy.pdf>
- [16] Ahmed H. Zewail. Femtochemistry: Atomic-Scale Dynamics of the Chemical Bond. *J. Phys. Chem. A*, 104:5660–5694, 2000.  
URL [http://jafar.media.mit.edu/library/date\\_author\\_sorted/00.04.zewail.pdf](http://jafar.media.mit.edu/library/date_author_sorted/00.04.zewail.pdf)